The EUMETSAT Network of Satellite Application Facilities

ROM SAF
Radio Occultation Meteorology

ROM SAF CDOP-2

Visiting Scientist Report 28:

A new software tool for reducing systematic residual ionospheric errors in GNSS-RO level 3 products

Matthew Angling
University of Birmingham

Danish Meteorological Institute (DMI)
European Centre for Medium-Range Weather Forecasts (ECMWF)
Institut d'Estudis Espacials de Catalunya (IEEC)
Met Office (METO)

Ref: SAF/ROM/DMI/REP/VS/28
Version: 1
Date: 16 December 2016

DOCUMENT AUTHOR TABLE

	Author(s)	*Function*	*Date*	*Comment*
Prepared by:	Matthew Angling	ROM SAF Visiting Scientist	15/12/2016	
Reviewed by (internal):	Sean Healy	ROM SAF Local Manager	15/12/2016	
Approved by:	Kent B. Lauritsen	ROM SAF Project Manager	16/12/2016	

DOCUMENT CHANGE RECORD

Issue/Revision	*Date*	*By*	*Description*
Draft 0.1	02/12/2016	MJA	First draft
0.2	15/12/2016	MJA	Delivered report
1.0	16/12/2016	MJA	Version 1

VS Author

The VS study was carried out by Prof. Matthew Angling, University of Birmingham; Email: M.Angling@bham.ac.uk

VS Duration

The VS study was performed during June - December 2016 at the home institute of the candidate with two visits to ECMWF.

ROM SAF

The Radio Occultation Meteorology Satellite Application Facility (ROM SAF) is a decentralised processing center under EUMETSAT which is responsible for operational processing of GRAS radio occultation (RO) data from the Metop satellites and radio occultation data from other missions. The ROM SAF delivers bending angle, refractivity, temperature, pressure, humidity, and other geophysical variables in near-real time for NWP users, as well as reprocessed data (Climate Data Records) and offline data for users requiring a higher degree of homogeneity of the RO data sets. The reprocessed and offline data are further processed into globally gridded monthly-mean data for use in climate monitoring and climate science applications.

The ROM SAF also maintains the Radio Occultation Processing Package (ROPP) which contains software modules that aids users wishing to process, quality-control and assimilate radio occultation data from any radio occultation mission into NWP and other models.

The ROM SAF Leading Entity is the Danish Meteorological Institute (DMI), with Cooperating Entities: i) European Centre for Medium-Range Weather Forecasts (ECMWF) in Reading, United Kingdom, ii) Institut D'Estudis Espacials de Catalunya (IEEC) in Barcelona, Spain, and iii) Met Office in Exeter, United Kingdom. To get access to our products or to read more about the ROM SAF please go to: http://www.romsaf.org

Intellectual Property Rights

List of Contents

Executive Summary

The standard approach to remove the effects of the ionosphere is to estimate a corrected neutral atmosphere bending angle from a combination of the L1 and L2 bending angles as described by [*Vorob'ev and Krasil'nikova*, 1994]. This approach is known to result in systematic errors that increase as a function of the electron density squared, integrated over the vertical profile. Consequently, [*Healy and Culverwell*, 2015] and [*Danzer et al.*, 2015] have proposed an extension to the standard ionospheric correction that is dependent on the squared L1/L2 bending angle difference and a scaling term (κ).

The variation of κ with height, time, season, location and solar activity (i.e. the f10.7 flux) has been investigated by applying a 1D bending angle operator to electron density profiles provided by a monthly median ionospheric climatology model. As expected, the residual bending angle is well correlated (negatively) with the vertical TEC. However, κ is more strongly dependent on the solar zenith angle. Furthermore, over the height range of interest (40-80 km) κ is approximately linear with height.

Using a random selection of vertical profiles from the NeQuick (spanning 1960 to 2010) the median κ is 14 rad^{-1} . A simple κ model has also been developed. It is independent of ionospheric measurements, but incorporates geophysical dependencies (i.e. solar zenith angle, solar flux, altitude). Both the scalar and modelled κ are an improvement over using a κ of zero. In the case of the modelled κ, the mean error (i.e. bias) and the standard deviation of the residual errors are reduced to -2.2×10^{-10} rad and 2.0×10^{-9} rad respectively. Although the scalar κ also reduces bias for the global average the selected value of κ (14 rad^{-1}) is only appropriate for a small band of locations around the solar terminator. In the day time, the scalar κ is consistently too high and this results in an over correction of the bending angles and a positive bending angle bias. Similarly, in the night time, the scalar κ is too low. However, in this case, the bending angles are already small and the impact of the choice of κ is less pronounced

It is recommended that the ROM SAF should:

- Assess the sensitivity of level 3 climatologies to the bending angle bias and standard deviation bounds determined by the current study. Furthermore, the magnitude of other error terms (i.e. non-symmetry [*Zeng et al.*, 2016]) should be assessed in light of these results.
- Encourage climate re-processing centres to implement scalar and model kappa methods for improving the ionospheric bending angle corrections and assess the outcome.
- Seek ways to work with climate re-processing centres to determine an effective validation strategy of the bending angle corrections. This may involve development of an end-to-end ray-trace utilising statistical realisations of the ionosphere (including perturbations from travelling ionospheric disturbances, etc). Alternatively an ionospheric data assimilation scheme (for example AENeAS [*Angling and Elvidge*, 2016]) could be used to provide more realistic representations of the ionosphere.

1. Introduction

1.1 Contractual background

This report forms part of the Task 2 deliverable of the ROM SAF CDOP-2 Visiting Scientist Proposal No. 28: A new software tool for reducing systematic residual ionospheric errors in GNSS-RO level 3 products (ROM_AVS16_03).

The objectives of the VS project are:

- Modify the pre-existing python software tool, which currently computes the L1 and L2 bending angles from the NeQuick ionospheric electron density model, to compute residual ionospheric errors and the kappa (κ) parameter associated with an improved ionospheric correction. The software package will be standalone and will include a version of the NeQuick ionospheric electron density model.
- Use the software tool to assess the spatial and temporal variability of the residual ionospheric errors, expanding on the work in [*Danzer et al.*, 2015], and to quantify the errors associated with a simple approximation such as κ=14. Develop and test a new fast κ model, and compare with both the NeQuick results and a simple scalar approach.

1.2 Technical background

[*Kursinski et al.*, 1997] provides an outline of the Global Navigation Satellite System radio occultation (GNSS-RO) technique. In the case of the Global Positioning System (GPS), the GPS satellites transmit on two L-band channels (L1, L2) at $f_1 = 1575.42$ MHz and $f_2 = 1227.60$ MHz and the signals are received by a satellite in low earth orbit (LEO) (Figure 1).

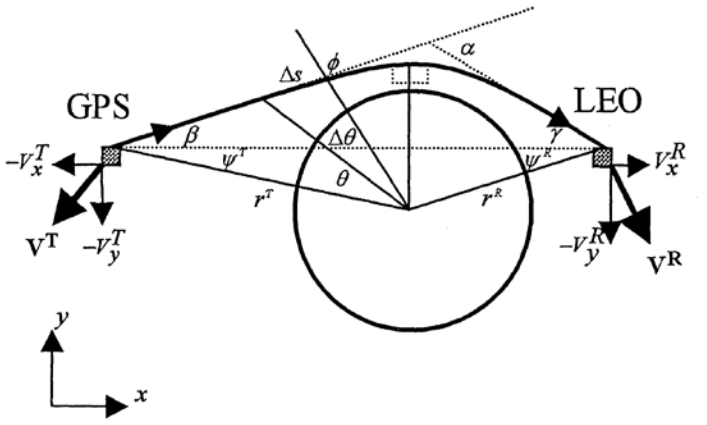

Figure 1. Radio occultation geometry. Reproduced from [Healy, 2001]

Assuming spherical symmetry, the bending angle of the ray between the GPS satellite and a receiver in LEO is:

$$\alpha_{Li}(a) = -2a \int_{r_t}^{\infty} \frac{dn_i/dr}{n_i\sqrt{(n_i r)^2 - a^2}} dr \qquad \text{Equation 1}$$

where $i = 1,2$ depending on the frequency; a is the impact parameter; r_t is the tangent height of the ray path; and n_i is the refractive index. The impact parameter is given by:

$$a = nrsin(\phi) = const \qquad \text{Equation 2}$$

To a first order approximation, the refractive index comprises terms dependent on the neutral atmosphere refractivity (N_n), the ionospheric electron density (n_e), and the frequency (f) squared:

$$n_i \cong 1 + 10^{-6}N_n(r) - 40.3\frac{n_e(r)}{f_i^2} \qquad \text{Equation 3}$$

Therefore, the measured L1 and L2 bending angles are different from each other, and both contain neutral and ionospheric components. The standard approach taken in operational RO processing centres is to estimate a corrected neutral atmosphere bending angle (α_c) using the approach described by [*Vorob'ev and Krasil'nikova*, 1994] (herein referred to as VK94):

$$\alpha_c(a) = \alpha_{L1}(a) + \frac{f_2^2}{f_1^2 - f_2^2}[\alpha_{L1}(a) - \alpha_{L2}(a)] \qquad \text{Equation 4}$$

where the L1 and L2 bending angles (α_{L1} and α_{L2} respectively) are interpolated to a common impact parameter. One benefit of this approach is that it is based on the standard parameters estimated by the retrieval system and does not require *a priori* information about the ionosphere. One downside is that a systematic bending angle error remains. [*Vorob'ev and Krasil'nikova*, 1994] showed that these errors increase as a function of the electron density squared, integrated over the vertical profile.

These residual ionospheric errors vary with the solar cycle and have been recognised as a potential source of bias in the ROM SAF level 3 climatology products [*Danzer et al.*, 2013]. Recent work by the ROM SAF team, combined with the ROM SAF Visiting Scientist Activity 24 conducted by Dr Danzer (University of Graz) [*Danzer*, 2014; *Danzer et al.*, 2015; *Healy and Culverwell*, 2015], has led to a proposed modification of the standard GPS-RO ionospheric correction for climate applications.

[*Healy and Culverwell*, 2015] have proposed a modification to the standard ionospheric correction of the form:

$$\alpha_c(a) = \alpha_{L1}(a) + \frac{f_2^2}{f_1^2 - f_2^2}[\alpha_{L1}(a) - \alpha_{L2}(a)] + \kappa(a)(\alpha_{L1}(a) - \alpha_{L2}(a))^2 \qquad \text{Equation 5}$$

where the κ term compensates for the systematic residual error in the standard approach. An appropriate value for κ has been investigated using simple analytic functions for the ionosphere [*Healy and Culverwell*, 2015] and using a raytracer through a 3D ionospheric model [*Danzer et al.*, 2015], though it should be noted that this study was limited to a low latitude band because of noise in the simulation system. It has been shown that κ generally falls in the range of 10 to 20 rad^{-1} and a simple scalar model, $\kappa \sim 14$, provides a good first approximation, improving the accuracy of the "dry" temperature retrievals [*Danzer et al.*, 2015]. Nevertheless, it is clear that κ will vary as a function of height, time, season,

location and solar activity and therefore it is possible that existing ionospheric climatology models could be used to compute an improved correction term by modelling the monthly mean, temporal and spatial variations of κ more realistically.

The aim of the current project is to investigate the variation of κ with height, time, season, location and solar activity (i.e. the f10.7 flux). This has been done by applying a 1D bending angle operator to electron density profiles provided by the NeQuick monthly median ionospheric climatology model [*Nava et al.*, 2008]. As well as examining the variations in κ, a "fast kappa model" has been developed. It is independent of ionospheric measurements, but does incorporate the relevant geophysical dependencies (i.e. solar zenith angle, solar flux).

1.3 Report structure

The document is organized as follows:

- Section 2: Description of the spatial, temporal and geophysical variations of κ
- Section 3: Development of a fast model of κ
- Section 4: Description of the software (NeQuick, 1D observation operator, κ model)
- Section 5: Conclusions and recommendations

2. Kappa variations

2.1 Introduction

A month median 3D ionospheric model (in this case NeQuick) and a 1D bending angle operator (both described in more detail in Section 4) can be used to estimate the residual ionospheric error and thereby estimate values for κ. The VK94 corrected bending angle is given by

$$\alpha_c(a) = \alpha_{L1}(a) + \frac{f_2^2}{f_1^2 - f_2^2}[\alpha_{L1}(a) - \alpha_{L2}(a)] + \Delta\alpha \qquad \text{Equation 6}$$

where $\Delta\alpha$ is the residual ionospheric error. In each of the examples shown in the following sections the same basic procedure has therefore been followed:

1. Use NeQuick to estimate a vertical profile of electron density
2. Convert the electron density (n_e), to the refractive index (n_i) using the 1st order approximation ($n_i = 1 - 40.3 n_e / f_i^2$) for each frequency (L1 and L2)
3. Estimate bending angle using the 1D observation operator for L1 and L2
4. Form the VK94 corrected bending angle (α_c).

Since no neutral atmosphere is included in the estimate of the refractive index, α_c should be zero if VK94 provided a perfect correction. Any non-zero values are representative of the residual ionospheric error $\Delta\alpha$. The residual error is modelled as:

$$\Delta\alpha = \kappa(a)(\alpha_{L1}(a) - \alpha_{L2}(a))^2 \qquad \text{Equation 7}$$

And this the bending angles are known, this can be rearranged to provide an estimate of κ:

$$\kappa(a) = \frac{\Delta\alpha}{(\alpha_{L1}(a) - \alpha_{L2}(a))^2} \qquad \text{Equation 8}$$

The main area of interest for κ estimation is between 40 and 80 km. It is in this region where the residual error from the ionospheric correction is likely to be a major contributor to the overall error budget.

2.2 Height dependence

The Figure 2 to Figure 5 show two examples of the vertical electron density profile, the L1/L2 bending angles, the residual error and κ. The test parameters are given in Table 1. Over the height range of interest (40-80 km), Figure 5 shows that κ is approximately linear, but its gradient is dependent on the local time.

Parameter	Test 1	Test 2
Latitude	50°	50°
Longitude	0°	0°
Time	12 UT	00 UT
Month	June	June
f10.7	150	150

Table 1. Test parameters for height dependence examples

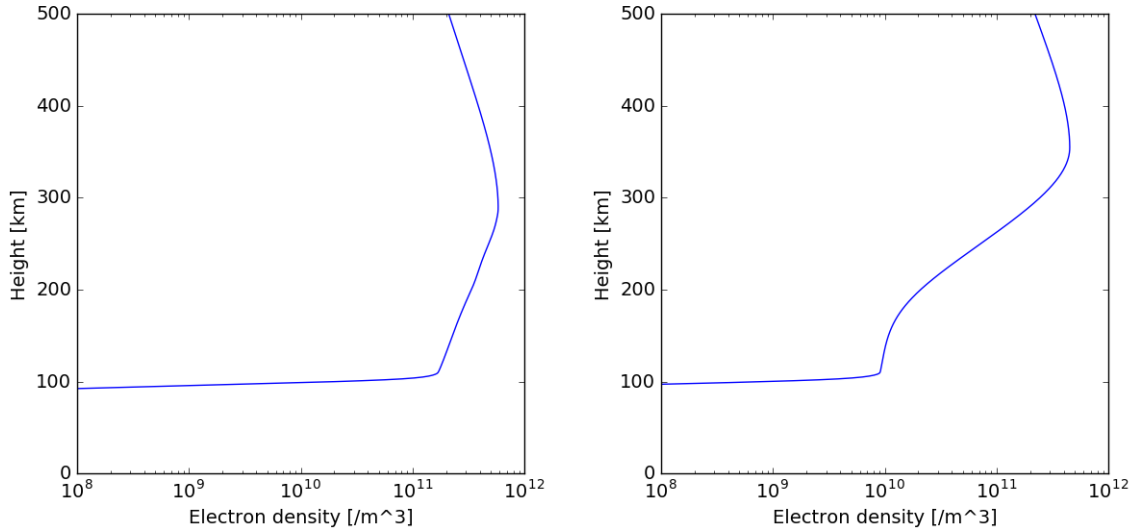

Figure 2. Electron density profiles for test 1 (left, midday) and test 2 (right, midnight)

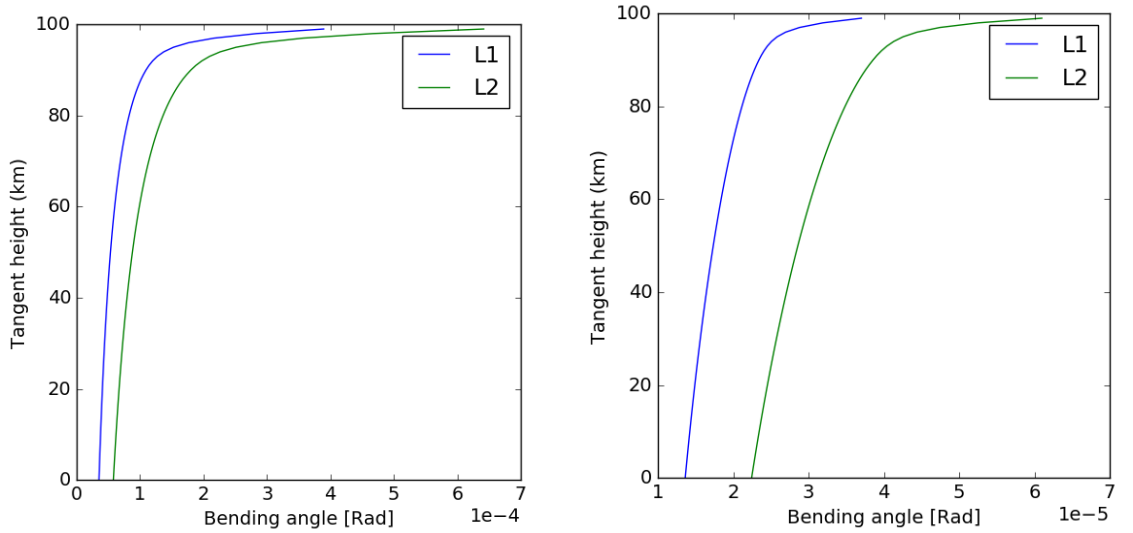

Figure 3. L1 and L2 bending angles for test 1 (left, midday) and test 2 (right, midnight)

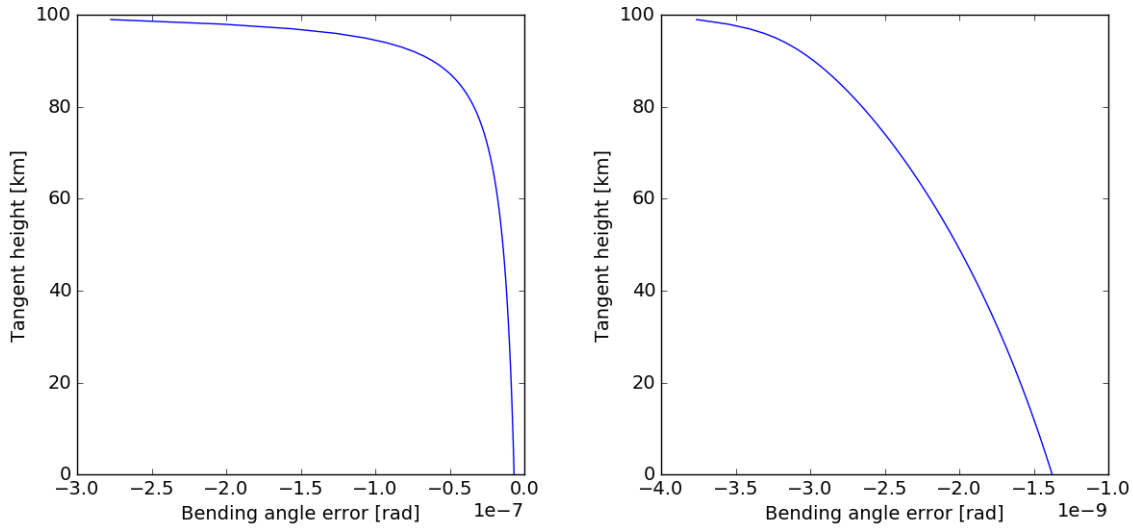

Figure 4. Bending angle residual errors for test 1 (left, midday) and test 2 (right, midnight)

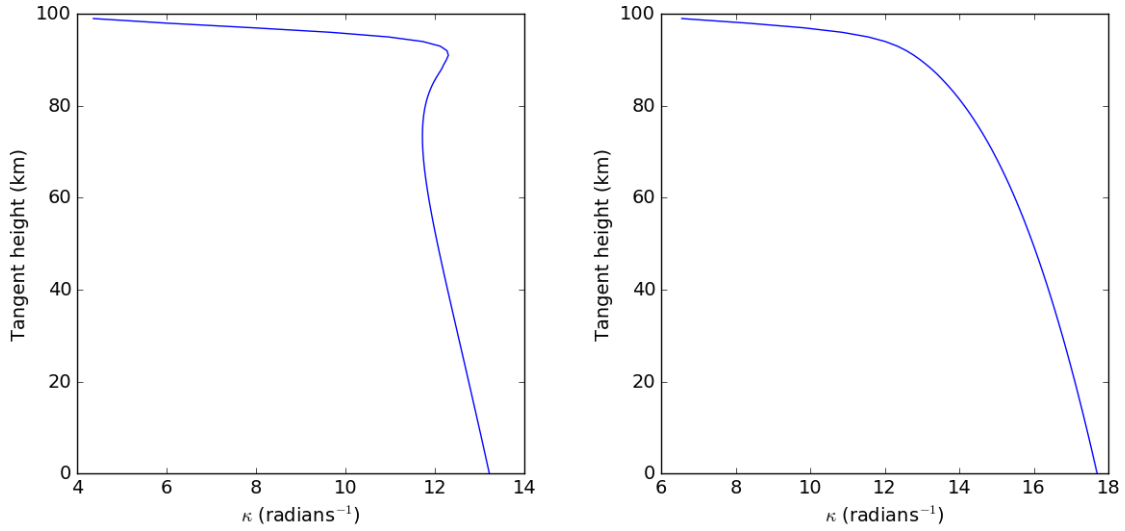

Figure 5. Estimate of κ for test 1 (left, midday) and test 2 (right, midnight)

2.3 Geographic dependence

The geographic dependence of bending angle correction can be demonstrated by plotting maps of the TEC (Figure 6), residual bending angle (Figure 7) and κ (Figure 8). In this case the test parameters are given in Table 2. As expected, the residual bending angle is well correlated (negatively) with the vertical TEC. However, the κ appears to be more strongly dependent on the solar zenith angle.

Parameter	Test 1	Test 2
Latitude	-85 to 85°	-85 to 85°
Longitude	-180 to 180°	-180 to 180°
Time	12 UT	12 UT
Month	June	December
f10.7	150	150
Tangent height	60 km	60 km

Table 2. Geographic test parameters.

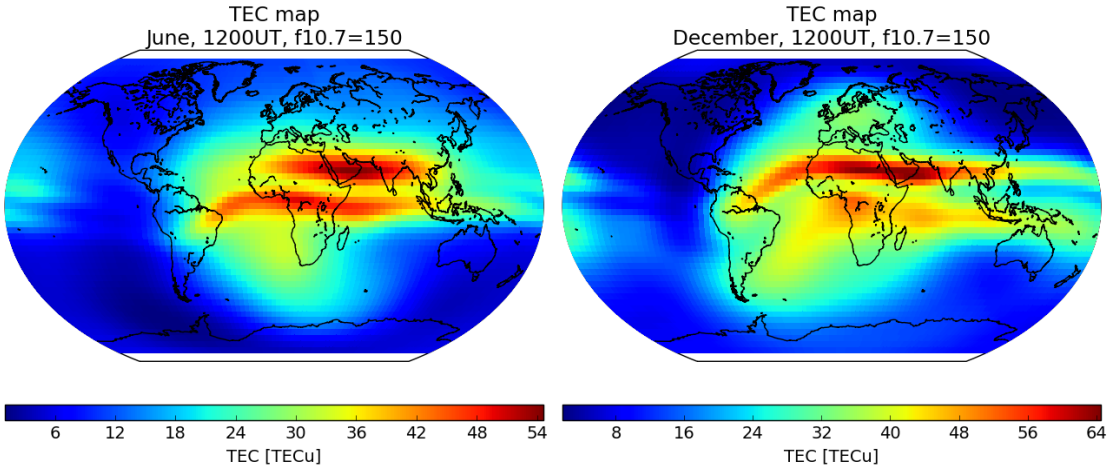

Figure 6. Vertical TEC from NeQuick for 12 UT, f10.7=150, June (left) and December (right).

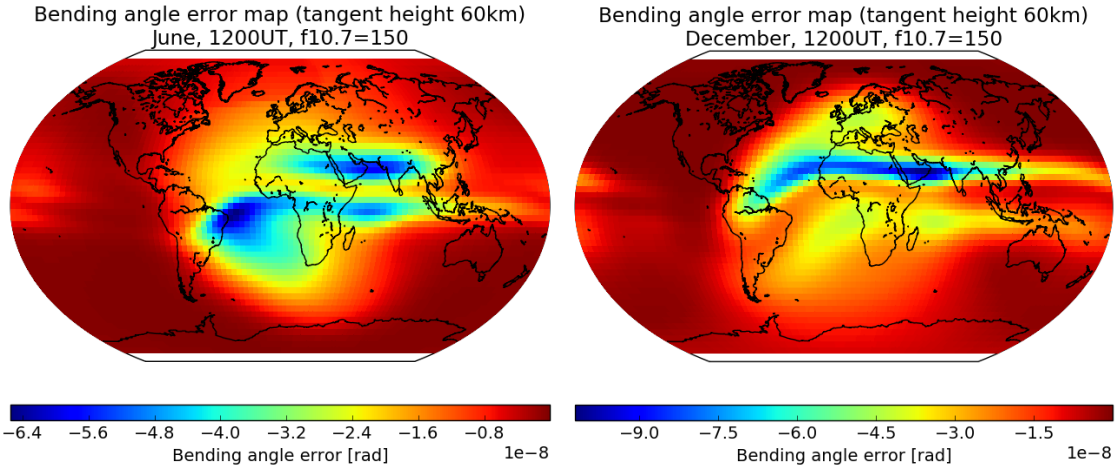

Figure 7. Estimated residual bending angle error for 12 UT, f10.7=150, June (left) and December (right).

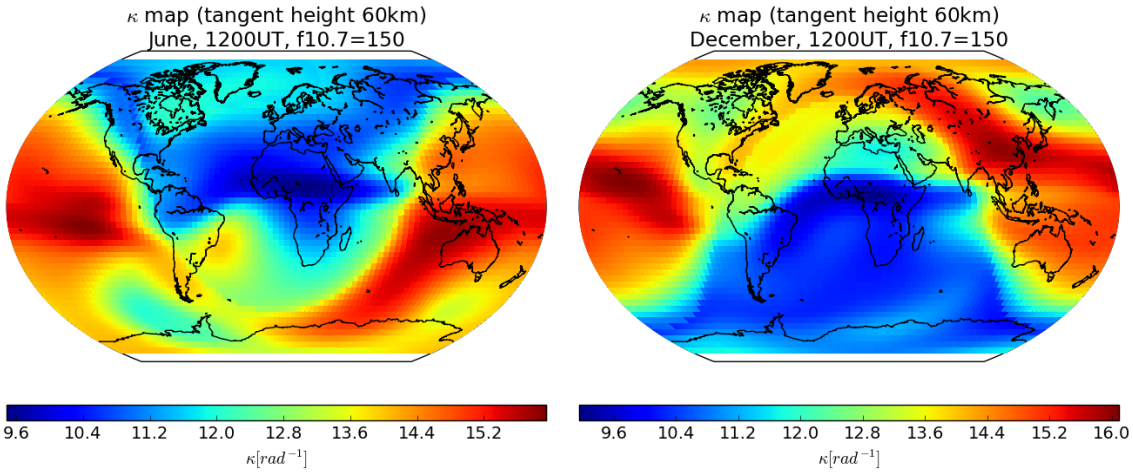

Figure 8. Estimated κ for 12 UT, f10.7=150, June (left) and December (right).

2.4 Solar cycle dependence

The solar cycle dependence of κ has been investigated by estimating κ at a tangent height of 60 km above London for each day over the last 60 years (Table 3). The results (Figure 9) show that κ is negatively correlated with f10.7; i.e. κ is low when the vertical TEC is large which occurs when f10.7 is high. Furthermore the dynamic range of κ is considerably smaller than that of the f10.7 (and hence TEC and bending angle), varying by a factor of approximately 50% compared to approximately 300% for f10.7

Parameter	Value
Latitude	51.5°
Longitude	-0.128°
Time	12 UT
Tangent height	60 km

Table 3. Solar cycle test parameters.

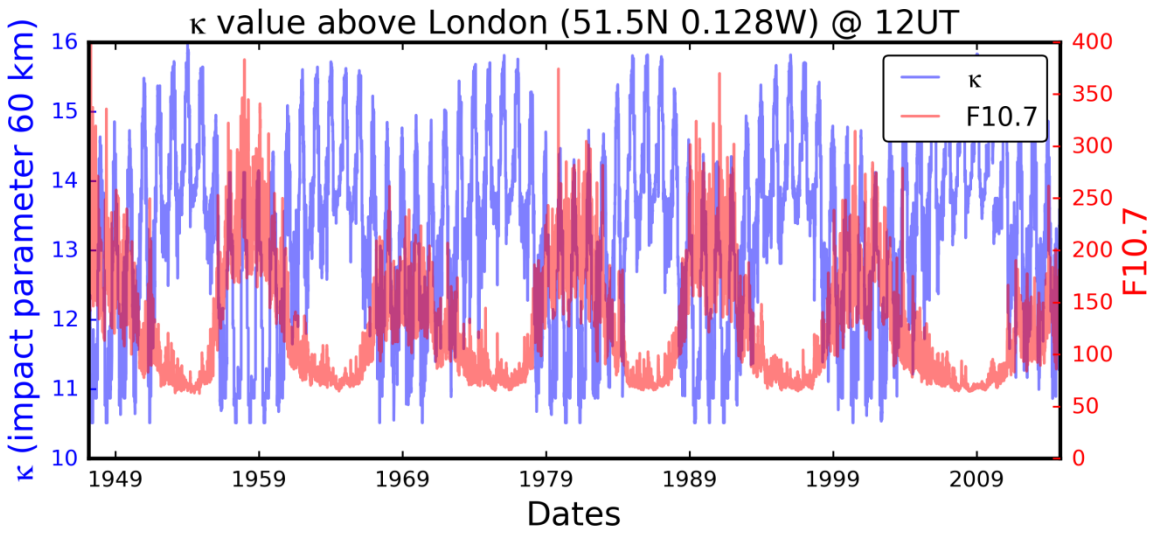

Figure 9. Solar cycle dependence of κ.

3. Models of κ

3.1 Introduction

Section 2 has presented examples of how κ can vary spatially and with solar cycle. In this section simple models of κ will be assessed in order to evaluate their potential to reduce the residual bending angle errors in the VK94 correction. Three models will be considered:

- κ equals zero; this represents the current situation with the unmodified VK94 correction
- κ is a scalar; this is the approach proposed by [*Healy and Culverwell*, 2015]
- κ is a function of latitude, longitude, solar zenith angle and solar flux.

In order the build the models a set of 25000 κ estimates where generated from NeQuick using random drivers (uniformly distributed over the ranges in Table 4). The true solar flux is used for each randomly selected day/year.

Parameter	Range
Latitude	-80 to 80°
Longitude	-180 to 180°
Time	0 to 23 UT
Day of year	1 to 365
Year	1960 to 2010
Tangent height	40 to 80 km

Table 4. Parameter ranges for random κ generation.

A further independent set of 25000 κ estimates were also generated using the same random parameter ranges to act as a set data set.

3.2 Scalar κ

The random κ values are shown in Figure 10. The median value is marked by the horizontal line and has value of 14 rad^{-1}. This value is used as the scalar model.

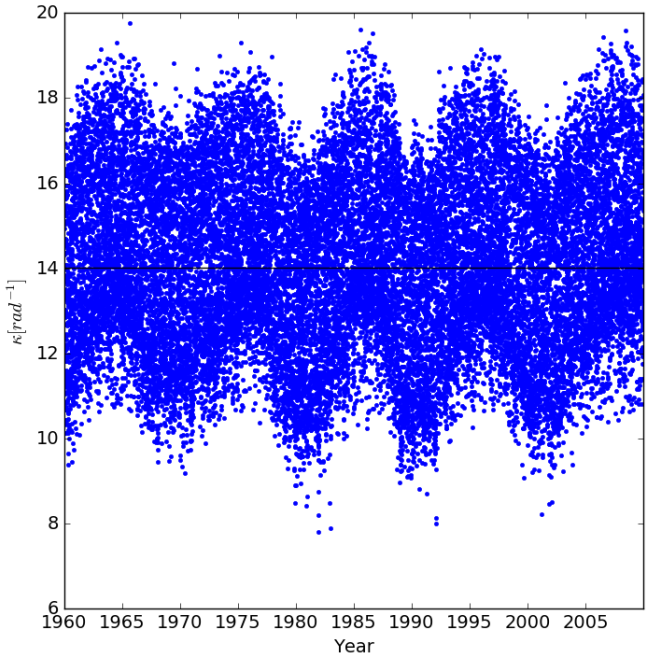

Figure 10. Random κ values. The horizontal line marks the median (=14 rad^{-1}).

3.3 Functional form κ

The aim of this model is to produce a very simple functional form that mimics some of the response of κ that is not accounted for by the scalar model. Figure 8 is suggestive that κ is a function of solar zenith angle – this is a convenient parameter to use since it embodies the position, local time and season. Figure 11, Figure 12 and Figure 13 show κ as a function of solar zenith angle, f10.7 and altitude respectively. The figures indicate linear dependencies in all cases; therefore the following model is proposed:

$$\kappa = a + bf_{10.7} + c\chi + dh \qquad \text{Equation 9}$$

Where $f_{10.7}$ is the f10.7 flux (sfu), χ is the solar zenith angle (rad) and h is the height above the ground (km); a, b, c, d are scalars to be found by fitting the model to the data.

The Python code curve_fit from the scipy.optimize package has been used to fit the model. The parameter results and the associated variances are shown in Table 5. A plot of the NeQuick estimated κ compared to the modelled κ is shown in Figure 14. Figure 15 shows the geographic distribution of κ at 12 UT in June and December at 60 km altitude and with an f10.7 of 150. These maps can be directly compared with those in Figure 8.

Parameter	Units	Estimated value	variance of the parameter estimate
a	rad^{-1}	15.05	1.764×10^{-3}
b	rad^{-1}.sfu^{-1}	-1.243×10^{-2}	1.786×10^{-8}
c	rad^{-2}	2.372	1.099×10^{-4}
d	rad^{-1}.km^{-1}	-5.332×10^{-2}	3.351×10^{-7}

Table 5. Estimated model parameters and associated variances

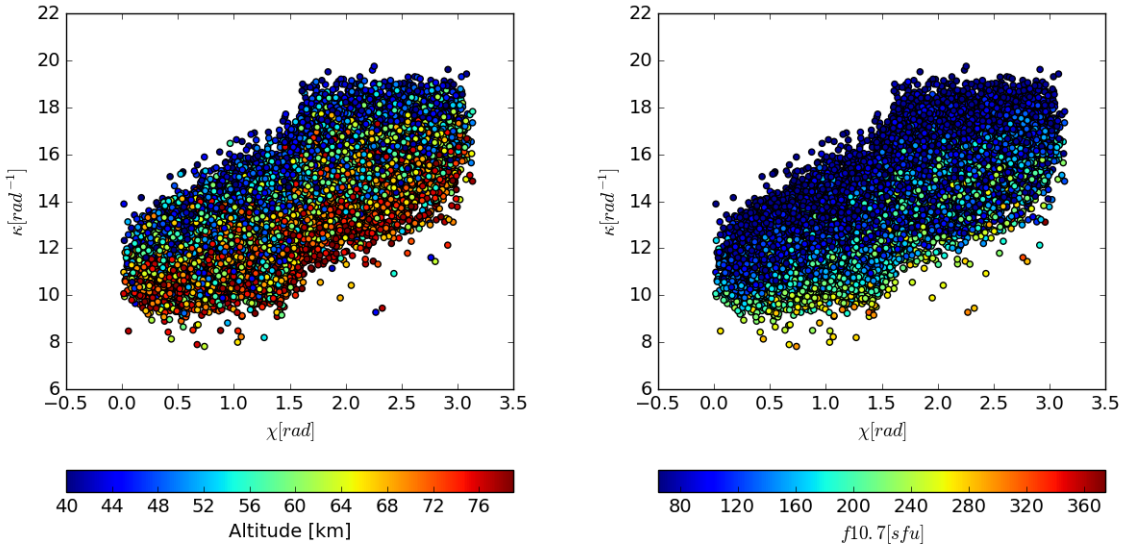

Figure 11. κ vs. solar zenith angle, colour coded by altitude (left) and f10.7 (right)

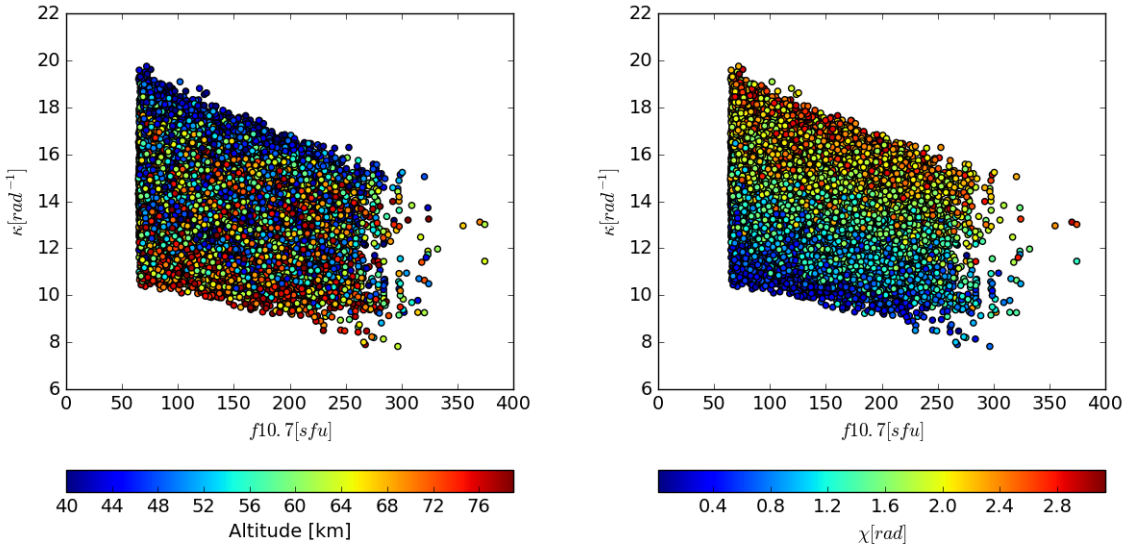

Figure 12. κ vs. f10.7, colour coded by altitude (left) and solar zenith angle (right)

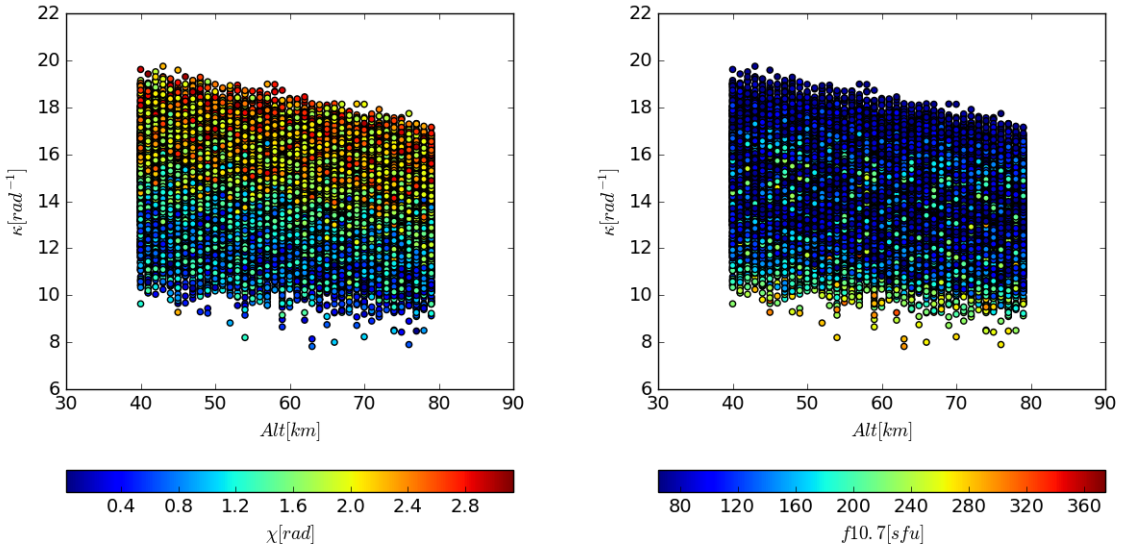

Figure 13. κ vs. altitude, colour coded by solar zenith angle (left) and f10.7 (right)

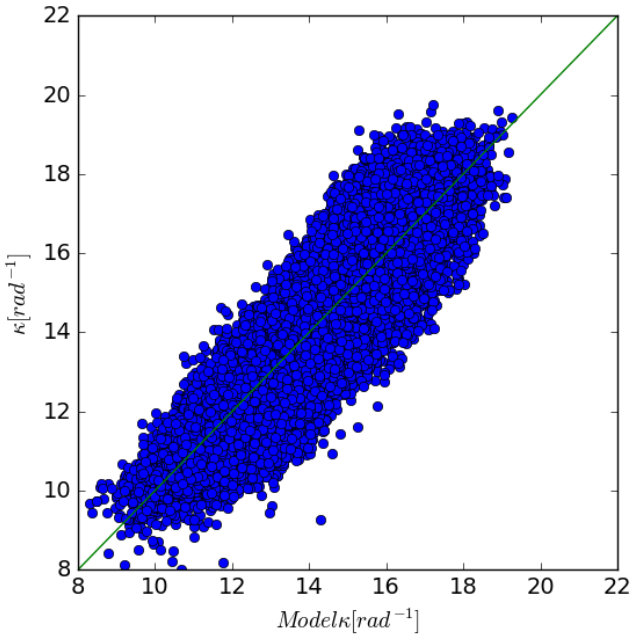

Figure 14. Scatter plot of κ estimated from NeQuick compared to modelled κ.

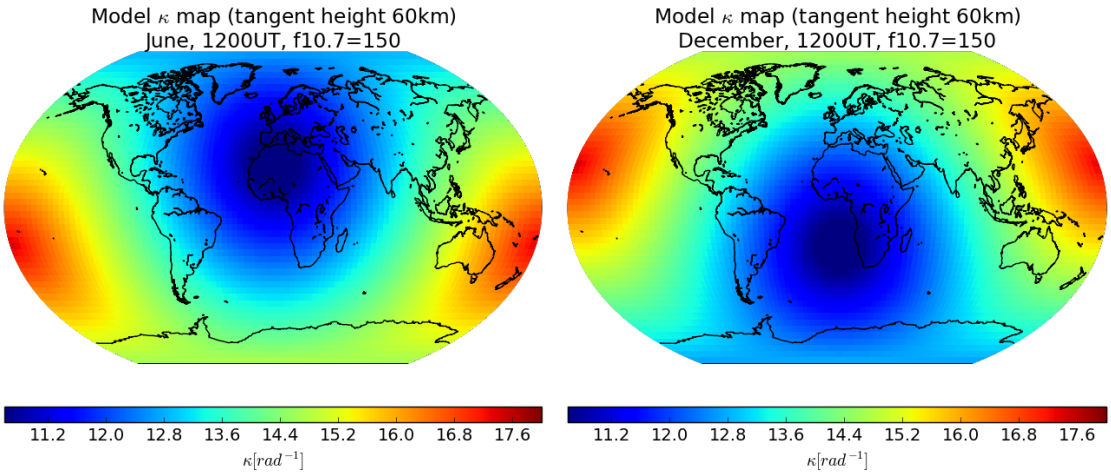

Figure 15. κ model for 12 UT, f10.7=150, June (left) and December (right). c.f. Figure 8.

3.4 Bending angle error reduction

The second set of 25000 randomly distributed points has been used to assess the reduction in residual bending angle for each of the κ models (zero, scalar and modelled). A scatter plot of the NeQuick κ and the modelled κ is shown in Figure 16. Figure 17 shows a histogram of the residual bending angle error. The bending angle error statistics are in Table 6.

Model	Mean (rad)	Median (rad)	Standard deviation (rad)
Zero κ	-1.3×10^{-8}	-4.5×10^{-9}	2.2×10^{-8}
Scalar (14) κ	1.5×10^{-9}	3.6×10^{-13}	5.4×10^{-9}
Model κ	-2.2×10^{-10}	5.6×10^{-13}	2.0×10^{-9}

Table 6. Global bending angle errors for three models

Both the scalar and modelled κ reults are an improvement over the zero κ results. In the case of the modelled κ, both the standard deviation and the mean error (i.e. bias) of the residual errors is reduced by an order of magnitude. Although the scalar κ also reduces bias for the global average, the geographic distribution of makes it clear that the selected value of κ (14 rad^{-1}) is only really appropriate for a small band of locations around the solar terminator (the line that separates the day side from the night side of the Earth). The effect of this is clear if the residual error statistics are considered for day time and night time separately.

Figure 18 and Figure 19 show histograms for residual bending angle for day and night respectively. In the day time, the scalar κ is consistently too high and this results in an over correction of the bending angles and a positive bending angle bias (Table 7). Similarly, in the night time, the scalar κ is too low. However, in this case, the bending angles are already small and the impact of the choice of κ is less pronounced (Table 8).

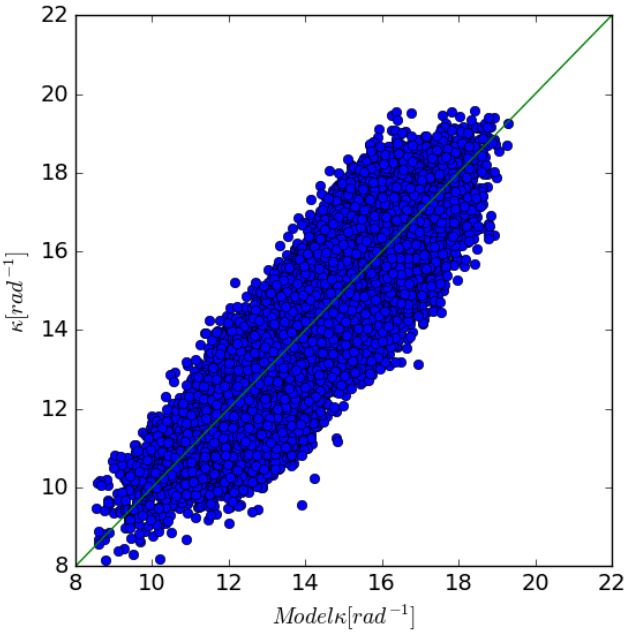

Figure 16. Scatter plot of NeQuick κ and modelled κ. c.f. Figure 14.

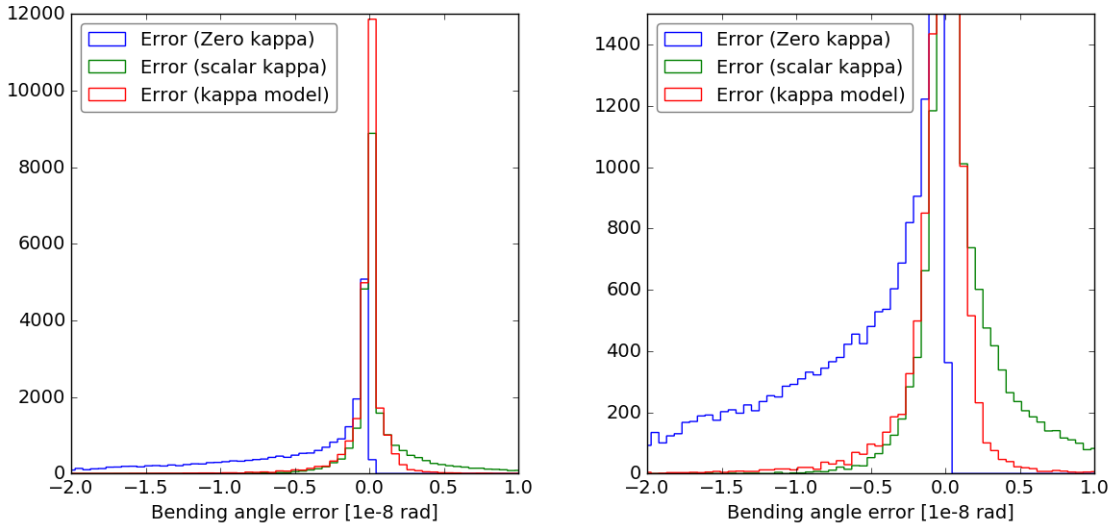

Figure 17. Histograms of globally distributed bending angle errors for zero κ, scalar κ, and modelled κ. Right: full histogram; left: zoomed to highlight tails.

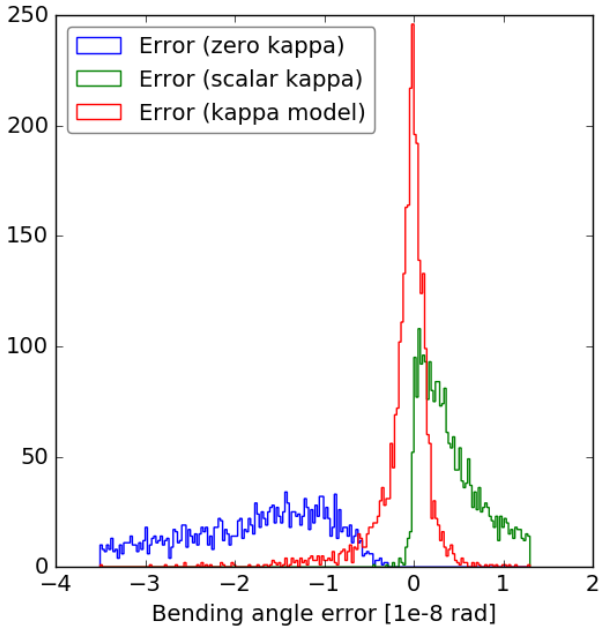

Figure 18. Histograms of day time bending angle errors for zero κ, scalar κ, and modelled κ.

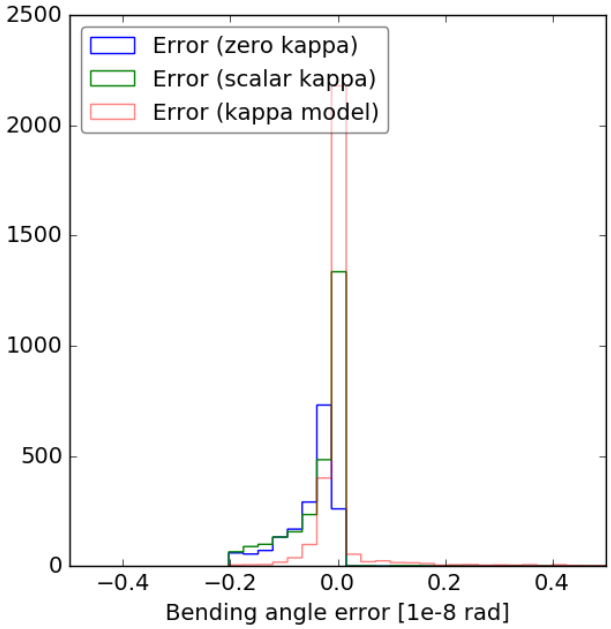

Figure 19. Histograms of night time bending angle errors for zero κ, scalar κ, and modelled κ.

Model	Mean (rad)	Median (rad)	Standard deviation (rad)
Zero κ	-3.3×10^{-8}	-2.3×10^{-8}	2.9×10^{-8}
Scalar (14) κ	7.6×10^{-9}	4.2×10^{-9}	9.9×10^{-9}
Model κ	-9.8×10^{-10}	-3.0×10^{-10}	3.4×10^{-9}

Table 7. Day time bending angle errors for three models

Model	Mean (rad)	Median (rad)	Standard deviation (rad)
Zero κ	-7.9×10^{-9}	-1.0×10^{-9}	2.3×10^{-8}
Scalar (14) κ	-7.0×10^{-10}	-1.5×10^{-10}	2.1×10^{-9}
Model κ	1.7×10^{-10}	6.2×10^{-12}	1.9×10^{-9}

Table 8. Night time bending angle errors for three models

4. Software description

4.1 NeQuick

NeQuick is an monthly median ionospheric electron density model developed at the Aeronomy and Radiopropagation Laboratory (now Telecommunications/ICT for Development Laboratory) of the Abdus Salam International Centre for Theoretical Physics (ICTP), Trieste, Italy, and at the Institute for Geophysics, Astrophysics and Meteorology (IGAM) of the University of Graz, Austria [*Nava et al.*, 2008]. The model is based on the Di Giovanni - Radicella (DGR) model [*Di Giovanni and Radicella*, 1990] which was modified for the PRIME project in COST 238 to provide electron densities from ground to 1000 km. The model has been designed to have continuously integrable vertical profiles which allows for rapid calculation of the TEC for trans-ionospheric propagation applications. The current versions NeQuick can be run up to a height of 20000 km and is used in the Galileo GNSS system to calculate ionospheric corrections [*Angrisano et al.*, 2013].

NeQuick is a "profiler" which makes use of three profile anchor points at the E layer peak, the F1 peak, and the F2 peak. To specify the anchor points it uses the layer critical frequencies (foE, foF1, foF2) and the F2 maximum usable frequency factor (M3000(F2)) [*Davies*, 1965]. foE is determined using a solar zenith angle model; foF1 is assumed to be proportional to foE during daytime and zero during nighttime; and foF2 and M3000(F2) are derived from the ITU-R (CCIR) coefficients in the same way as the International Reference Ionosphere (IRI) [*Bilitza and Reinisch*, 2008].

Between 100 km and the peak of the F2 layer, NeQuick uses an electron density profile based on the superposition of five semi-Epstein layers [*Epstein*, 1930; *Rawer*, 1983]; i.e. the Epstein layers have different thickness parameters for their top and bottom sides. The topside of NeQuick is a simplified approximation to a diffusive equilibrium. A semi-Epstein layer represents the model topside with a height-dependent thickness parameter that has been empirically determined.

4.2 Model variants

There are three primary variants of the NeQuick model (Table 9).

Variant	Version/ date	Notes
ITU	May 2002	International Telecommunication Union Radiocommunication Sector (ITU-R) standard P.531 recommends the use of NeQuick to provide electron density values for trans-ionopsheric modelling. The FORTRAN software is available from: http://www.itu.int/en/ITU-R/study-groups/rsg3/ionotropospheric/Electron%20density%20distribution%20(NeQuick2).zip
ICTP	v2.0.2 Nov 2010	ICTP continue to develop NeQuick. FORTRAN code is available on request from Bruno Nava (bnava@ictp.it)
NeQuick G		NeQuick G is the variant used in Galileo receivers. A reference implementation is not available. However, details of the model are given in the following documents: http://www.gsc-europa.eu/galileo-reference-documents/ionospheric-model http://www.gsc-europa.eu/sites/default/files/sites/all/files/ERRATASHEET1_final_for Publication.pdf

Table 9. NeQuick variants

The model used in the current project is the University of Birmingham's translation of the NeQuick v2.0.2 from FORTRAN into Python. Very minor (negligible) differences in results are observed due to the use of different interpolation routines. The Python code has been largely vectorised to increase the speed of operation. Further enhancements are been included in a version 3 (Table 10). Version 3 has been used in the current work.

Feature	v2.0.2	UoB, v3
f10.7	Clipped to: 63 < f10.7 < 193 This is the ITU recommendation for use with the ITU ionospheric coefficients	Clipped to: 63 < f10.7 Seems to provide better TEC performance during high f10.7 solar cycle peaks.
Day of month	Not used	The day of month is used to linearly interpolate between two monthly coefficient files. This prevents step changes in electron density at month boundaries
hmE	Hard coded to 120 km	Hard coded to 110 km. This is a more reasonable value. However, a more sophisticated model should be implemented in future; i.e. [*Chu et al.*, 2009].
Bottom side taper	Displays a discontinuity at 90 km that can produce artefacts in bending angle estimations	Bottomside taper added using a tanh function.

Table 10. Updates to produce v3.

4.3 NeQuick User guide

4.3.1 Files

Two files are required to run NeQuick (Table 11). Both files should be placed in the same directory in the Python path.

File	Description
nequick.py	Python file containing model code and examples
data.h5	hdf5 file containing the ITU/CCIR ionospheric coefficients and the mapping from geographic coordinated to modified dip angle

Table 11. Files required to run NeQuick

4.3.2 Dependencies

The Python code has been developed using the Anaconda distribution (https://www.continuum.io/downloads). The packages listed in Table 12 are required.

Package	Module
numpy	
datetime	
os	
mpl_toolkits	basemap
h5py	
matplotlib	pyplot
mpl_toolkits.axes_grid1	make_axes_locatable

Table 12. NeQuick dependencies

4.3.3 Input parameters

The NeQuick input parameters are listed in Table 13.

Internally, NeQuick converts between f10.7 and the 12 month sunspot number (R_{12}) thus:

$$f10.7 = 63.7 + 8.9 \times 10^{-4} R_{12}^2 + 0.728 R_{12} \qquad \textit{Equation 10}$$

$$R_{12} = \sqrt{167273 + 1123.6(f10.7 - 63.7)} - 408.99 \qquad \textit{Equation 11}$$

F10.7 values can be obtained from the indices files available at:

ftp://ftp.ngdc.noaa.gov/STP/GEOMAGNETIC_DATA/INDICES/KP_AP

For convenience, a text file (F10.7_historical.txt) has been supplied with this document that contains f10.7 from 1947 to 2014 in the format YYYYMMDD FFF.F

Parameter	Type	Description	Default value
along	M	Geographic longitude (degrees E)	
alat	M	Geographic latitiude (degrees N)	
h	M	Height (km) Can be 1D or 3D. If 3D must have dimensions of nlon × nlat × nalt	
mth	M	month (1 .. 12)	
flx	M	10.7 cm solar radio flux (flux units) Can be: scalar 1D if grid==False (same length as lon) 2D if grid==True (same dimension as nlon × nlat)	
UT	M	Universal Time (hours)	
grid	O	True/False. If True, a nlon × nlat × nalt output grid is formed from the along, alat, h inputs	False
version	O	2 = NeQuick 2.0.2 or 3 = UoB v3	3
day	O	day (1 .. 28/30/31) Only used in version 3	15
foF2	O	Array of foF2 values (dimension nlon x nlat) If used it replaces the calculated foF2 values	None
foF1	O	Array of foF1 values (dimension nlon x nlat) If used it replaces the calculated foF1 values	None
foE	O	Array of foE values (dimension nlon x nlat) If used it replaces the calculated foE values	None
hmF2	O	Array of hmF2 values (dimension nlon x nlat) If used it replaces the calculated hmF2 values	None
hmF1	O	Array of hmF1 values (dimension nlon x nlat) If used it replaces the calculated hmF1 values	None
hmE	O	Array of hmE values (dimension nlon x nlat) If used it replaces the calculated hmE values	None
hdf	O	Name/location of HDF file containing CCIR and MODIP values. If not set, the individual files are used.	None
botTaper	O	Specified the width of the bottomside taper. Set to None to have no tapering	3

Table 13. Python NeQuick input parameters. M=Mandatory, O=Optional

4.3.4 Example programmes

Eight example programmes are included in the nequick.py source file (Table 14).

Name	Description/Call
example1	Produce a 3D grid of electron density neq = example1()
example2	Produce a single height profile using gridded output (Figure 20) neq = example2()
example3	Produce a grid using gridded solar flux neq = example3()
example4	Get electron density along a straight line and calculate TEC tec = example4()
example5	Compare version 2 and version 3 TECs tec2, tec3 = example5()
example6	Map of electron density at 300km (Figure 21) neq = example6()
example7	Test passing peak parameters to vertical profile (Figure 22) neq1, neq2 = example7()
example8	Test passing peak parameters to grid neq = example8()

Table 14. Example routines showing how to use the NeQuick routines

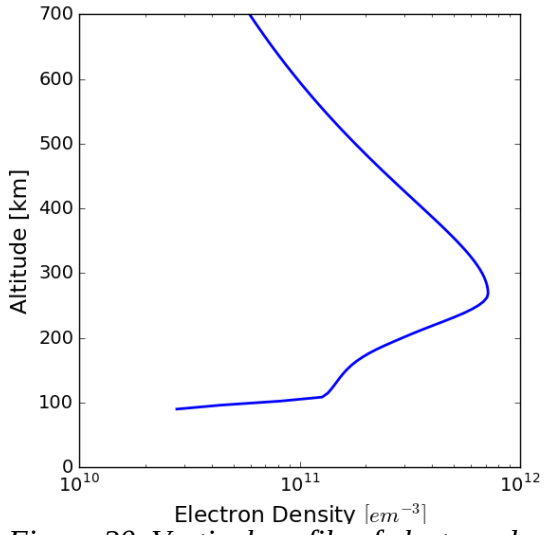

Figure 20. Vertical profile of electron density generated using example2.

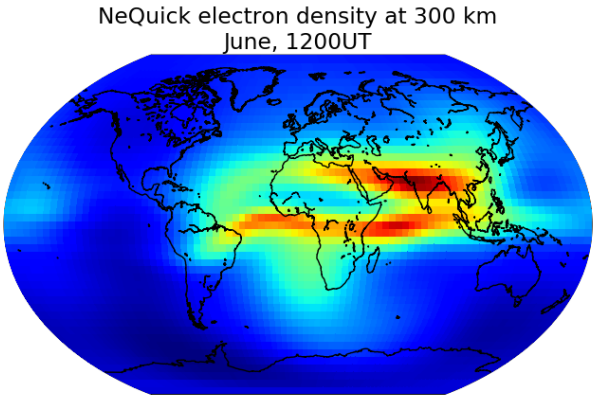

Figure 21. Map of electron density generated using example6.

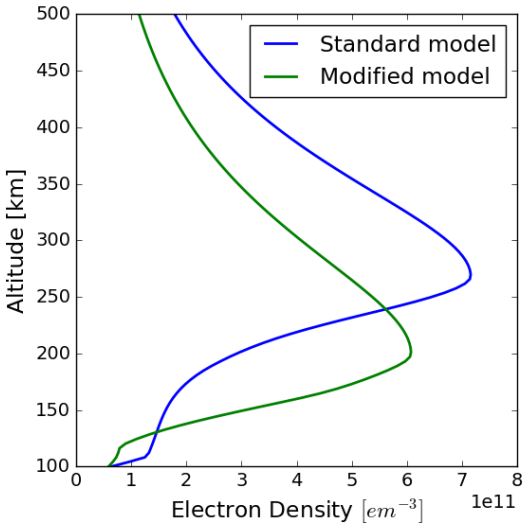

Figure 22. Vertical profile of electron density generated using example7. The modified model has had peak parameters passed in to replace the standard values.

4.4 Observation operator

Python routines have been written to calculate the frequency dependent bending angle, the post-correction bending angle residuals and kappa. All equations have been taken from [*Healy and Culverwell*, 2015].

4.4.1 Files

A single file is required to run the bending angle routines (Table 15).

File	Description
gpsro.py	Python file containing bending angle routines

Table 15. Files required to run bending angle routines

4.4.2 Dependencies

The Python code has been developed using the Anaconda distribution (https://www.continuum.io/downloads). The packages listed in Table 16 are required.

Package	Module
numpy	
scipy	
nequick	
matplotlib	pyplot
mpl_toolkits	basemap
mpl_toolkits	axes_grid1

Table 16. gpsro.py dependencies

4.4.3 Subroutines

Four subroutines are included in gpsro.py (Table 17)

Routine	Description
bending_angle	To estimate the 1D bending angle from a vertical profile of electron density.
bending_residual	To estimate the residual bending angle after ionospheric correction.
corrected_bending_angle	To estimate the corrected bending angle using the approach of [*Vorob'ev and Krasil'nikova*, 1994]
kappa	To estimate the value of kappa, given prior estimates of the bending angles and the bending angle residual (Figure 23)
vert_test	To produce plots showing vertical profiles of electron density, bending angle, residual bending angle and κ
geo_test	To produce maps showing TEC, residual bending angle and κ

Table 17. Bending angle and associated routines.

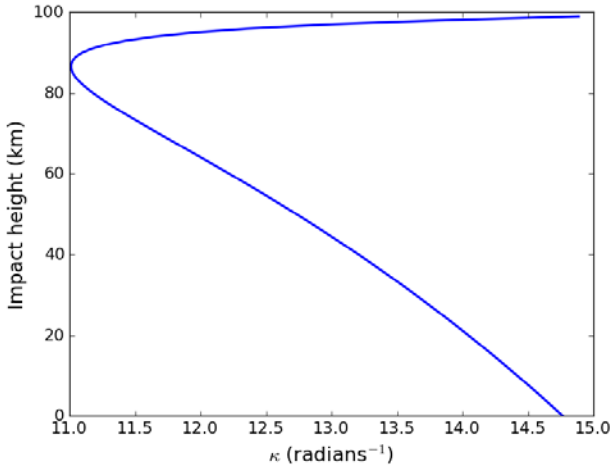

Figure 23.κ estimated from a vertical electron density profile produced by NeQuick (0°E, 30°N, June, f10.7=150) and the 1D bending angle residuals.

4.5 Kappa model

Python routines have been written to calculate the fast κ model using the parameters given in Section 3.3.

4.5.1 Files

A single file is required to run the κ model routines (Table 18).

File	Description
kappa_model.py	Python file containing kappa model routines

Table 18. Files required to run κ model routines

4.5.2 Dependencies

The Python code has been developed using the Anaconda distribution (https://www.continuum.io/downloads). The packages listed in Table 19 are required.

Package	Module
numpy	
matplotlib	pyplot
pickle	
mpl_toolkits	basemap
mpl_toolkits	axes_grid1

Table 19. kappa_model.py dependencies

4.5.3 Subroutines

Four subroutines are included in kappa_model.py (Table 20)

Routine	Description
kappa_model	Calcualre the value of the fast kappa model given position, time and solar flux
solarZenithAngle	To estimate the solar zenith angle. Required by kappa_model
map_kappa_model	To produce a map of kappa at a particular time/date, altitude and solar flux (eg Figure 15)
kGlobalResiduals	To estimate the global residual bending angle error based on the data in the pickle file test_kappa.p
kLocalResidualsNight	To estimate the night time residual bending angle error based on the data in the pickle file test_kappa.p
kLocalResidualsNight	To estimate the day time residual bending angle error based on the data in the pickle file test_kappa.p

Table 20. κ model and associated routines.

5. Conclusions and recommendations

5.1 Conclusions

The standard approach to remove the effects of the ionosphere is to estimate a corrected neutral atmosphere bending angle from a combination of the L1 and L2 bending angles as described by [*Vorob'ev and Krasil'nikova*, 1994]. This approach is known to result in systematic errors that increase as a function of the electron density squared, integrated over the vertical profile. Consequently, [*Healy and Culverwell*, 2015] and [*Danzer et al.*, 2015] have proposed an extension to the standard ionospheric correction that is dependent on the squared L1/L2 bending angle difference and a scaling term (κ).

Studies using simple analytic functions for the ionosphere [*Healy and Culverwell*, 2015] and using a raytracer through a 3D ionospheric model [*Danzer et al.*, 2015] have shown that κ generally falls in the range of 10 to 20 rad^{-1} and that a simple scalar model, $\kappa \sim 14$, provides a good first approximation. Nevertheless, it is clear that κ will vary as a function of height, time, season, location and solar activity and therefore ionospheric climatology models could be used to compute an improved correction term by modelling the monthly mean, temporal and spatial variations of κ more realistically.

The variation of κ with height, time, season, location and solar activity (i.e. the f10.7 flux) has been investigated by applying a 1D bending angle operator to electron density profiles provided by the NeQuick monthly median ionospheric climatology model [*Nava et al.*, 2008]. In particular, the behaviour of κ between 40 and 80 km has been considered as this is the region where bending angle errors may be large compared with the bending angles themselves. As expected, the residual bending angle is well correlated (negatively) with the vertical TEC. However, κ is more strongly dependent on the solar zenith angle. Furthermore, over the height range of interest κ is approximately linear with height, but its rate of change is clearly dependent on the local time.

Using a random selection of vertical profiles from the NeQuick (spanning 1960 to 2010) the median κ is 14 rad^{-1}. This agrees well with the result from [*Healy and Culverwell*, 2015]. A simple κ model has also been developed. It is independent of ionospheric measurements, but incorporates geophysical dependencies (i.e. solar zenith angle, solar flux, altitude). Both the scalar and modelled κ are an improvement over using a κ of zero. In the case of the modelled κ, the mean error (i.e. bias) and the standard deviation of the residual errors are reduced to -2.2×10^{-10} rad and 2.0×10^{-9} rad respectively. Although the scalar κ also reduces bias for the global average, the geographic distribution of makes it clear that the selected value of κ (14 rad^{-1}) is only appropriate for a small band of locations around the solar terminator. In the day time, the scalar κ is consistently too high and this results in an over correction of the bending angles and a positive bending angle bias. Similarly, in the night time, the scalar κ is too low. However, in this case, the bending angles are already small and the impact of the choice of κ is less pronounced

5.2 Recommendations

The residual bending angle errors produced by the ionosphere vary with the solar cycle and with local time. They have been recognised as a potential source of bias in the ROM SAF

level 3 climatology products [*Danzer et al.*, 2013]. It is therefore recommended that the ROM SAF should:

- Assess the sensitivity of level 3 climatologies to the bending angle bias and standard deviation bounds determined by the current study. Furthermore, the magnitude of other error terms (i.e. non-symmetry [*Zeng et al.*, 2016]) should be assessed in light of these results.
- Encourage climate re-processing centres to implement scalar and model kappa methods for improving the ionospheric bending angle corrections and assess the outcome.
- Seek ways to work with climate re-processing centres to determine an effective validation strategy of the bending angle corrections. This may involve development of an end-to-end ray-trace utilising statistical realisations of the ionosphere (including perturbations from travelling ionospheric disturbances, etc). Alternatively an ionospheric data assimilation scheme (for example AENeAS [*Angling and Elvidge*, 2016]) could be used to provide more realistic representations of the ionosphere.

6. References

Angling, M. J., and S. Elvidge (2016), On the use of the local ensemble transform Kalman filter (LETKF) for ionospheric data assimilation, in *13th European Space Weather Week*, Ostend, Belgium.

Angrisano, A., S. Gaglione, C. Gioia, M. Massaro, and S. Troisi (2013), Benefit of the NeQuick Galileo Version in GNSS Single-Point Positioning, *Int. J. Navig. Obs.*, *2013*, 1–11, doi:10.1155/2013/302947.

Bilitza, D., and B. W. Reinisch (2008), International Reference Ionosphere 2007: Improvements and new parameters, *J. Adv. Sp. Res.*, *42*(4), 599–609, doi:10.1016/j.asr.2007.07.048.

Chu, Y.-H., K.-H. Wu, and C.-L. Su (2009), A new aspect of ionospheric E region electron density morphology, *J. Geophys. Res.*, *114*(A12), A12314, doi:10.1029/2008JA014022.

Danzer, J. (2014), *Testing a new model for the residual ionospheric correction error in GPS radio occultation retrievals, CDOP-2, VS24*.

Danzer, J., B. Scherllin-Pirscher, and U. Foelsche (2013), Systematic residual ionospheric errors in radio occultation data and a potential way to minimize them, *Atmos. Meas. Tech.*, *6*(8), 2169–2179, doi:10.5194/amt-6-2169-2013.

Danzer, J., S. B. Healy, and I. D. Culverwell (2015), A simulation study with a new residual ionospheric error model for GPS radio occultation climatologies, *Atmos. Meas. Tech*, *8*, 3395–3404, doi:10.5194/amt-8-3395-2015.

Davies, K. (1965), *Ionospheric radio propagation*, National Bureau of Standards, USA.

Epstein, P. S. (1930), Reflection of Waves in an Inhomogeneous Absorbing Medium, *Proc. Natl. Acad. Sci.*, *16*(10).

Di Giovanni, G., and S. M. Radicella (1990), An analytical model of the electron density profile in the ionosphere, *Adv. Sp. Res.*, *10*(11), 27–30, doi:10.1016/0273-1177(90)90301-F.

Healy, S. B. (2001), Radio occultation bending angle and impact paramter errors caused by horizontal refractive index gradients in the troposhere: a simulation study, *JGR*, *106*(D11), 11875–11889.

Healy, S. B., and I. D. Culverwell (2015), A modification to the standard ionospheric correction method used in GPS radio occultation, *Atmos. Meas. Tech.*, *8*(8), 3385–3393, doi:10.5194/amt-8-3385-2015.

Kursinski, E. R., G. A. Hajj, J. T. Schofield, R. P. Linfield, and K. R. Hardy (1997), Observing Earth's atmosphere with radio occultation measurements using the Global Positioning System, *J. Geophys. Res.*, *102*(D19), 23429–23465.

Nava, B., P. Coisson, and S. Radicella (2008), A new version of the neQuick ionosphere electron density model, *J. Atmos. Solar-Terr. Phys.*, doi:10.1016/j.jatsp.2008.01.015.

Rawer, K. (1983), Replacement of the Present Sub-Peark Plasma Density Profile by a Unique Expression, *Adv. Sp. Res.*, *2*(10), 183–190.

Vorob'ev, V. V, and T. G. Krasil'nikova (1994), Estimation of the accuracy of the

atmospheric refractive index recovery from the NAVSTAR system, *USSR Phys. Atmos. Ocean (Eng. Trans.)*, *29*(5), 602–609.

Zeng, Z., S. Sokolovskiy, W. Schreiner, D. Hunt, J. Lin, and Y.-H. Kuo (2016), Ionospheric correction of GPS radio occultation data in the troposphere, *Atmos. Meas. Tech.*, *9*(2), 335–346, doi:10.5194/amt-9-335-2016.

7. List of Acronyms

1D	One dimensional
3D	Three dimensional
CCIR	International Radio Consultative Committee
COSMIC	Constellation Observing System for Meteorology, Ionosphere, and Climate
ECMWF	European Centre for Medium-range Weather Forecasts
EUMETSAT	EUropean organisation for the exploitation of METeorological SATellites
F10.7	Solar radio flux at 10.7 cm (2800 MHz)
foE/F1/F2	O-mode critical frequency of the E/F1/F2 layer
GNSS	Global Navigation Satellite System
GPS	Global Positioning System (USA)
GRAS	GNSS Receiver for Atmospheric Sounding (on Metop)
HDF	Hierarchical Data Format
hmE/F1/F2	Height of the maximum electron density in the E/F1/F2 layer
ICTP	Abdus Salam International Centre for Theoretical Physics
IGAM	Inst. for Geophysics, Astrophysics and Meteorology, University of Graz
ITU	International Telecommunications Union
LEO	Low Earth Orbit
Metop	Meteorological Operational Satellite
MODIP	Modified dip angle
NetCDF	Network Common Data Form
NWP	Numerical Weather Prediction
RO	Radio Occultation
ROM SAF	Radio Occultation Meteorology (ROM) Satellite Application Facility (SAF) (EUMETSAT)
TEC	Total Electron Content
UT	Universal Time
VK94	Vorob’ev and Krasil’nikova, 1994